NIST Technical Note 1891

A Self-Learning Algorithm for Temperature Prediction in a Single Family Residence

Farhad Omar
Steven T. Bushby

This publication is available free of charge from:
http://dx.doi.org/10.6028/NIST.TN.1891

National Institute of
Standards and Technology
U.S. Department of Commerce

NIST Technical Note 1891

A Self-Learning Algorithm for Temperature Prediction in a Single Family Residence

Farhad Omar
Steven T. Bushby
Energy and Environment Division
Engineering Laboratory

September 2015

This publication is available free of charge from:
http://dx.doi.org/10.6028/NIST.TN.1891

U.S. Department of Commerce
Penny Pritzker, Secretary

National Institute of Standards and Technology
Willie E. May, Under Secretary of Commerce for Standards and Technology and Director

Disclaimer

Certain commercial entities, equipment, or materials may be identified in this document in order to describe an experimental procedure or concept adequately. Such identification is not intended to imply recommendation or endorsement by the National Institute of Standards and Technology, nor is it intended to imply that the entities, materials, or equipment are necessarily the best available for the purpose.

National Institute of Standards and Technology Technical Note 1891
Natl. Inst. Stand. Technol. Tech. Note 1891, 35 pages (September 2015)
http://dx.doi.org/10.6028/NIST.TN.1891
CODEN: NTNOEF

Abstract

In order to develop effective control optimization strategies to manage residential electricity consumption in a smart grid environment, predictive algorithms are needed that are simple to implement, minimize custom configuration, and provide sufficient accuracy to enable meaningful control decisions. Two of the largest electrical loads in a typical residence are heating and air-conditioning. A self-learning algorithm for predicting indoor temperature changes is derived using a first-order lumped capacitance technique. The algorithm is formulated in such a way that key design details such as window size and configuration, thermal insulation, and airtightness that effect heat loss and solar heat gain are combined into effective parameters that can be learned from observation. This eliminates the need for custom configuration for each residence.

Using experimental data from the National Institute of Standards and Technology (NIST) Net-Zero Energy Residential Test Facility (NZERTF), it was demonstrated that an effective overall heat transfer coefficient and thermal time constant for the house can be learned from a single nighttime temperature decay test. It was also demonstrated that an effective solar heat gain coefficient can be learned without knowledge of the window area and orientation by application of a self-learning, sliding-window algorithm that accounts for seasonal variations and daily weather fluctuations. The resulting algorithm is shown to be able to predict indoor temperatures for a one-day time horizon using a solar irradiance and outdoor temperature forecast, and control decisions for operating a heat pump.

Keywords

Net zero energy house; net zero energy residential test facility; thermal model; lumped capacitance model; thermal time constant; overall heat transfer coefficient; moving window optimization; sliding window optimization; parameter learning; parameter fitting, parameter optimization

Acknowledgments

The authors wish to thank everyone involved in the Net Zero Residential Test Facility project. Special thanks are extended to Dan Veronica, Amanda Pertzborn, Vance Payne, Harrison Skye, and Mark Kedzierski.

Authors Information

Farhad Omar
Electrical Engineer, Mechanical Systems & Controls Group
Engineering Laboratory
National Institute of Standards and Technology
100 Bureau Drive, Mailstop 8631
Gaithersburg, MD, 20899
Tel: 301-975-4008
Email: farhad.omar@nist.gov

Steven T. Bushby
Leader of Mechanical Systems & Controls Group
Engineering Laboratory
National Institute of Standards and Technology
100 Bureau Drive, Mailstop 8631
Gaithersburg, MD, 20899
Tel: 301-975-5873
Email: steven.bushby@nist.gov

Contents

List of Figures

List of Tables

1. Introduction

Developing effective control strategies to manage residential electricity consumption in a smart grid environment requires predictive algorithms for all significant electrical loads that are simple to implement, minimize custom configuration, and provide enough accuracy to enable meaningful control decisions. In a smart grid environment, time-varying prices, demand response agreements, or possibly market-based transactions to buy or sell electricity, may significantly influence the cost of electricity consumption. Other key inputs to control decisions include weather and occupant choices.

Heating, ventilating, and air-conditioning (HVAC) is one of the largest electrical loads in a typical house. In order to evaluate control strategies that might involve preheating or precooling, temperature setbacks, or letting the temperature drift during peak price periods, it is important to be able to predict the resulting indoor air temperature changes. Many tools to simulate building energy use and comfort conditions have been developed that have this capability [1]. Although details vary, these tools require information about the location, orientation, windows, and other construction details of the house. They also require expertise in crafting a simulation. A simpler approach is needed to develop control strategies that might be used in a typical home.

In this work, a self-learning algorithm for temperature prediction in a single family residence was developed. The approach taken was to define a simple lumped capacitance model where key parameters for the model can be learned through observation instead of derived from in depth knowledge of the construction details. The algorithm was validated using performance measurements from the Net-Zero Energy Residential Test Facility (NZERTF), at the National Institute of Standards and Technology (NIST) in Gaithersburg, Maryland [2, 3]. The NZERTF is a 251 m^2 (2700 ft^2), four bedroom house with a detached garage built entirely with commercially available products. The exterior of the NZERTF is shown in Figure 1.

Figure 1. The NZERTF house exterior

2. Lumped Capacitance Model

In order to predict the interior air temperature of a house, a first order lumped capacitance model described in [4] is utilized. The house is assumed to be a single control volume with a uniform interior temperature. Figure 2 shows a schematic of the overall energy balance on a house.

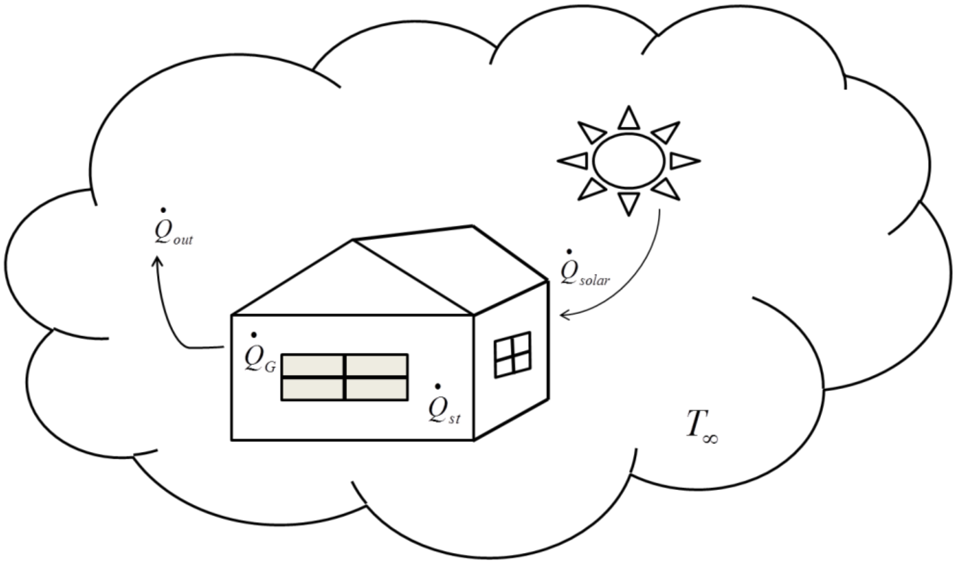

Figure 2. A house thermal energy balance

The energy balance equation as a rate of change of energy is given by:

$$\dot{Q}_{st} = \dot{Q}_{solar} + \dot{Q}_G - \dot{Q}_{out} \tag{1.1}$$

where:

$\dot{Q}_{st} = \frac{dQ_{st}}{dt} = \frac{dT}{dt}\rho V c_p$ is the rate of the thermal energy stored in the house;

ρ is the density;

c_p is the specific heat;

V is the volume;

$\dot{Q}_{Solar} = (q_{sol})$ is the total solar heat gain added to the house;

$\dot{Q}_G = (q_{hp} + q_l)$ is the internal heat generated inside the house by the heat pump (q_{hp}), and plug-loads (q_l) including sensible heat generated by the occupants; and

$\dot{Q}_{Out} = UA(T - T_{\infty})$ is the heat loss to the environment due to the temperature difference between the inside and the outside. *UA* is the overall heat transfer coefficient, *T* is the indoor dry-bulb and T_{∞} is the outside ambient dry-bulb temperatures, respectively. Note that radiation heat losses are neglected.

Applying these definitions, Equation (1.1) can be rewritten as follows:

$$\rho V c_p \frac{dT}{dt} = q_{sol} + q_{hp} + q_l - UA(T - T_{\infty}) \tag{1.2}$$

If we let $\psi = (T - T_{\infty})$, then $\frac{dT}{dt} = \frac{d\psi}{dt}$ and Equation (1.2) becomes:

$$\rho V c_p \frac{d\psi}{dt} = q_{sol} + q_{hp} + q_l - UA\psi \tag{1.3}$$

Dividing both side of Equation (1.3) by $\rho V c_p$ we obtain the following first-order differential equation:

$$\frac{d\psi}{dt} = \frac{q_{sol} + q_{hp} + q_l}{\rho V c_p} - \frac{UA\psi}{\rho V c_p} \tag{1.4}$$

Re-writing Equation (1.4):

$$\frac{d\psi}{dt} = b - a\psi \tag{1.5}$$

where:

$$a = \frac{UA}{\rho V c_p}, \text{and } b = \frac{q_{sol} + q_{hp} + q_l}{\rho V c_p}$$

Multiplying both sides of Equation (1.5) by an integrating factor e^{at} and rearranging gives:

$$e^{at}\frac{d\psi(t)}{dt} + e^{at}a\psi(t) = e^{at}b \tag{1.6}$$

Using the product rule, the left hand side of Equation (1.6) can be written as:

$$\frac{d}{dt}\left(e^{at}\psi\left(t\right)\right)=e^{at}b \tag{1.7}$$

Integrating both sides of Equation (1.7) with respect to *t* gives:

$$\begin{gathered}\int d\left(e^{at}\psi\left(t\right)\right)=\int e^{at}bdt\\ e^{at}\psi\left(t\right)=b\frac{1}{a}e^{at}+C\end{gathered} \tag{1.8}$$

Dividing both sides of Equation (1.8) by e^{at} gives:

$$\psi\left(t\right)=\frac{b}{a}+Ce^{-at} \tag{1.9}$$

when $t=0$, $C=\psi\left(0\right)-\frac{b}{a}$ then Equation (1.9) becomes:

$$\psi\left(t\right)=\frac{b}{a}+\left[\psi\left(0\right)-\frac{b}{a}\right]e^{-at} \tag{1.10}$$

Substituting the values for *a, b,* ψ back into the Equation (1.10) results in the first order lumped capacitance model. If we let $\psi(0)=T_i-T_\infty$ where T_i is the initial temperature of the house and T_∞ is the ambient temperature then Equation (1.10) becomes

$$T-T_\infty=\frac{q_{sol}+q_{hp}+q_l}{UA}+\left(T_i-T_\infty-\frac{q_{sol}+q_{hp}+q_l}{UA}\right)\exp\left(-\frac{UA}{\rho Vc_p}t\right) \tag{1.11}$$

Defining the thermal time constant τ such that:

$$\tau=\left(\frac{1}{UA}\right)\left(\rho Vc_p\right)$$

where:

$\left(\frac{1}{UA}\right)$ is the overall-lumped thermal resistance; and

$\left(\rho Vc_p\right)$ is the lumped thermal capacitance.

Re-writing and re-arranging Equation (1.11) gives the first order model to predict the interior temperature:

$$T = T_\infty + \frac{q_{sol} + q_{hp} + q_l}{UA} + \left(T_i - T_\infty - \frac{q_{sol} + q_{hp} + q_l}{UA} \right) \exp\left(-\frac{t}{\tau} \right) \tag{1.12}$$

The value of (q_{sol}) can be estimated from measurements of solar irradiance using methods discussed later in this document. The value of (q_l) is also known through a fixed occupancy schedule described in [3]. However, the values of *UA* and τ are not known a priori. A learning algorithm is used to estimate these values from measured data. In this paper they are denoted as effective quantities (UA_e, τ_e) to acknowledge the fact that the values are not the true *UA* and τ of the NZERTF but an approximation that will enable us to predict the indoor temperature.

A discrete form of Equation (1.12) is developed by defining t as $\Delta t = t_{k+1}$- t_k where $k = 1,2,\ldots,n$ are the discrete time steps and n is the number of data points. Let (Q_h = q_{sol} + q_{hp} + q_l) represent the total heat gain inside the NZERTF in every time step. Let T_i represent the indoor temperature. Applying these concepts to Equation (1.12) gives the one-step learning/prediction model:

$$T_{i,k+1} = T_{\infty,k} + \frac{Q_{h,k}}{UA_e} + \left(T_{i,k} - T_{\infty,k} - \frac{Q_{h,k}}{UA_e} \right) \exp\left(-\frac{\Delta t}{\tau_e} \right) \tag{1.13}$$

2.1 Learning the Overall Heat Transfer Coefficient and Thermal Time Constant

Estimates for the UA_e and τ_e are needed to use Equation (1.13) to predict the indoor temperature. Since both UA_e and τ_e are mainly driven by the temperature difference between the inside and outside, a single test was conducted in the NZERTF on a cold winter night. Testing at night eliminated the impact of direct solar heat gain into the interior space. During the test, the house's main thermostat setpoint was lowered to approximately 15.6 °C (60 °F), and the heat recovery ventilation unit was turned off. The first floor and outdoor dry-bulb temperatures were measured throughout the night. The first floor temperature is an average of measurements made in all the rooms on the first floor. Figure 3 shows the results of the test. The uncertainty in measuring the indoor and outdoor dry-bulb temperature described in [5], with a confidence level of 95 %, is ± 0.2 °C (0.4 °F) and ± 0.6 °C (1.0 °F), respectively.

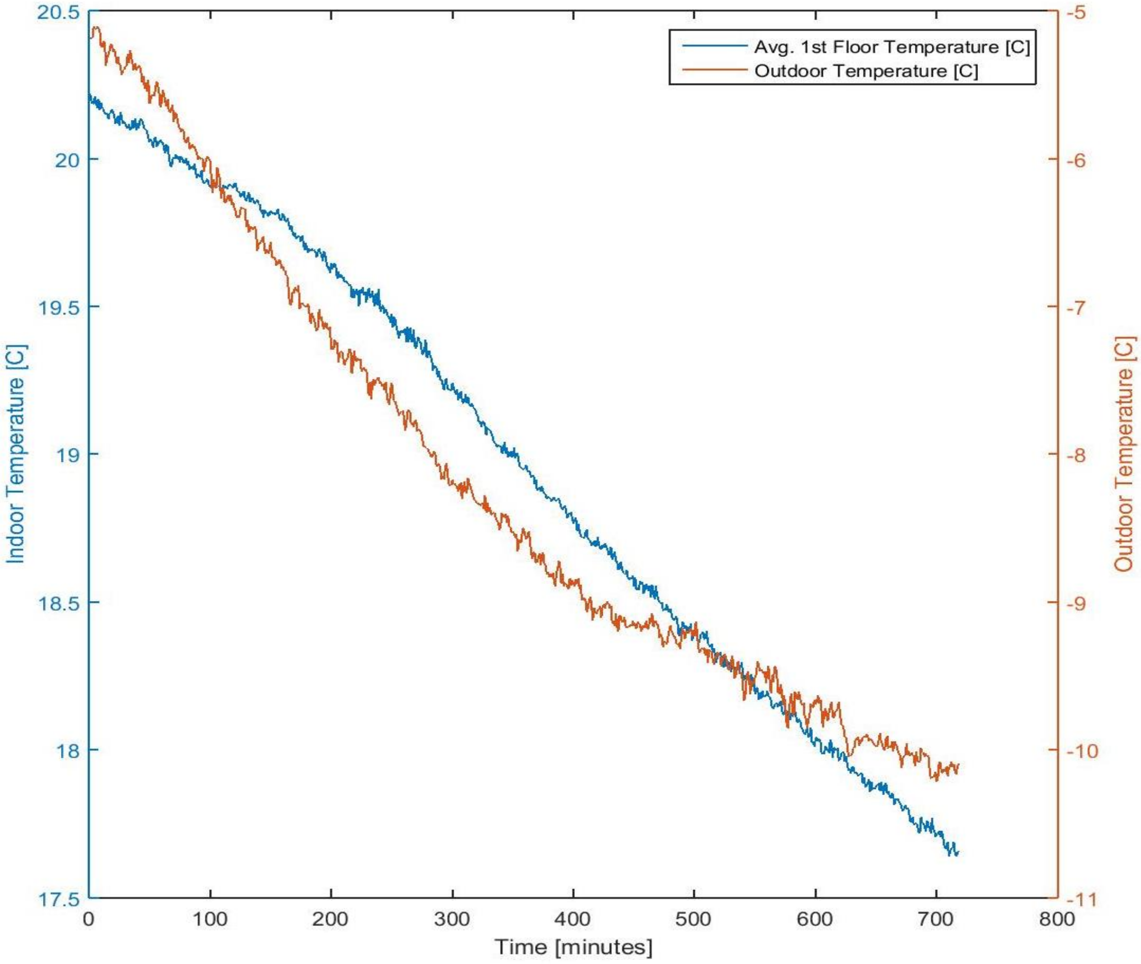

Figure 3. Results from a night temperature decay test

Because the heat pump energy and solar heat gain to the house are equal to zero in this test, Equation (1.13) is reduced to the following:

$$T_{i,k+1} = T_{\infty,k} + \frac{q_{l,k}}{UA_e} + \left(T_{i,k} - T_{\infty,k} - \frac{q_{l,k}}{UA_e} \right) \exp\left(-\frac{\Delta t}{\tau_e} \right) \tag{1.14}$$

In order to estimate UA_e and τ_e using an optimization technique, an objective function is defined as the sum of squared error (SSE) between the measured average first floor temperature (T_m) and the predicted temperature (T_p) obtained from Equation (1.14). The objective function is

$$f\left(UA_e, \tau_e\right) = \left\| T_m - T_p \right\|_2^2 \tag{1.15}$$

and, the optimization problem is:

$$\begin{aligned} &\min_{UA_e,\tau_e} \quad f\left(UA_e,\tau_e\right) \\ &1 \le UA_e \le \infty \\ &60 \le \tau_e \le \infty \end{aligned} \tag{1.16}$$

where, the units for upper and lower bounds of the UA_e are in W/K and τ_e are in minutes. For numerical stability, the lower bound of UA_e was set to 1; however, the upper bound was allowed to float because it was not known a priori. Similarly, the lower bound of τ_e was set to 1 hour and the upper bound was allowed float as well. A Matlab non-linear optimization function (*fmincon*) with its default interior-point algorithm was used to minimize Equation (1.16) subject to the upper and lower bound constraints. The result of the optimization is shown in Figure 4.

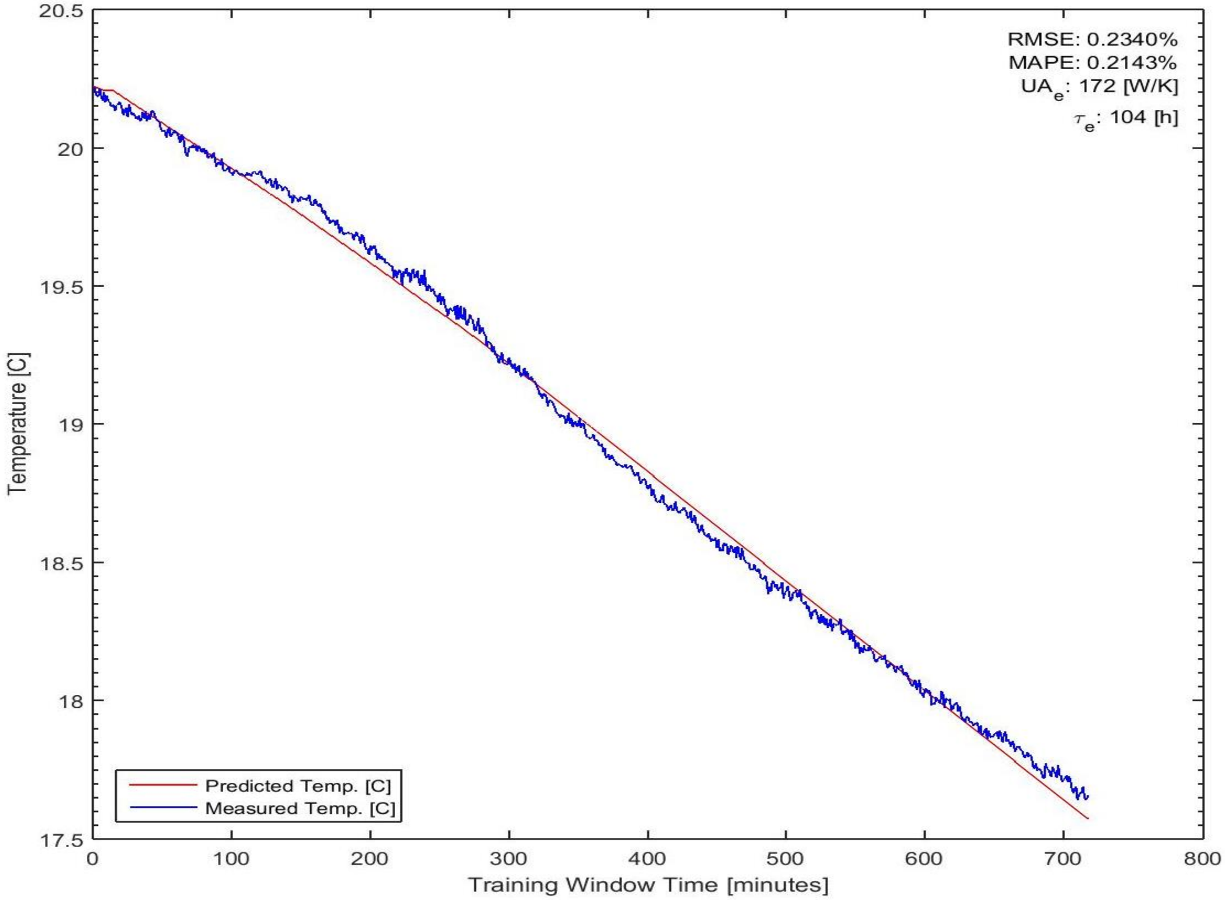

Figure 4. Comparison of predicted and measured first floor temperatures during a night test

Figure 4 shows the predicted and measured first floor temperature, for the test period, and statistics describing the goodness of fit. The resulting learned parameters are, UA_e = 172 W/K and τ_e = 104 h.

To verify the value of UA_e an alternative method was used to provide a comparison estimate. Daily heat pump thermal energy output for the period of October 2014 – May 2015 were plotted with respect to the indoor/outdoor temperature difference as shown in Figure 5. The uncertainty in measuring $T_{outdoor}$ and *Thermal Energy* described in [5], with a confidence level of 95 %, is ± 0.2 °C (0.4 °F) and ± 9.4 %, respectively. Assuming that internal loads and solar gain are small compared to the conductive and convective heat losses,

$$\dot{Q}_{hp} \approx UA\left(T_{\text{outdoor}} - T_{\text{setpoint}}\right)$$

Thus the slope of linear fit to the data provides an estimate for *UA*. From these data it was found that *UA = 180 ± 8 W/K* with a confidence of 95 %. This result confirms that learned value of UA_e = 172 W/K is a reasonable estimate.

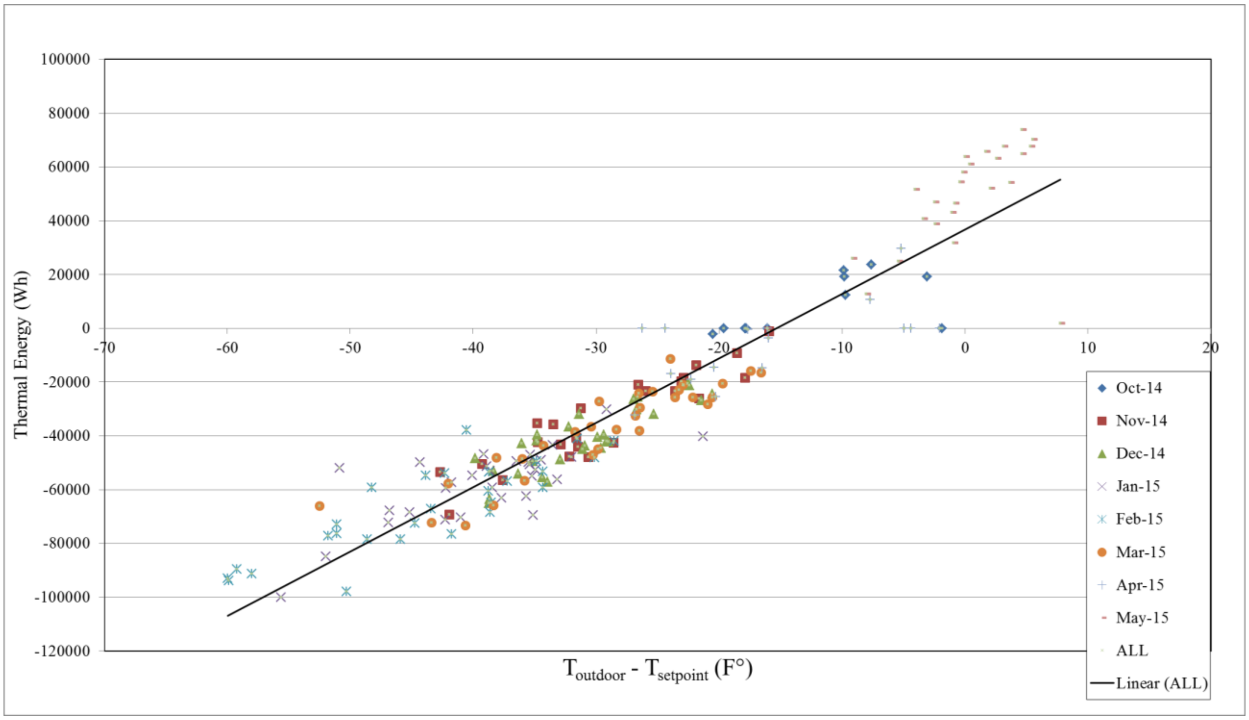

Figure 5. Heat pump load vs. temperature difference, courtesy of William V. Payne

2.3 Estimating Solar Gain

An estimate of solar heat gain is needed to apply Equation (1.13). Detailed procedures for estimating solar heat gain are provided in [6]. Modeling solar heat gain is a complex process that involves many details about window size, orientation, shading, and materials along with estimates of direct and indirect solar radiation. For the application intended in this work, these details are not likely to be available and the custom configuration needed to use them is not practical to obtain. The solution proposed is to develop a mathematical representation for solar heat gain with a small number of parameters that capture the unknown details, and then learn those parameter values by observation. One representation for solar heat gain is adapted from [7].

$$q_{sol} = E_{DN} \cos(\theta)(T - NA)W_A \tag{1.17}$$

where:

q_{sol} is the total solar heat gain;
E_{DN} is the direct normal irradiance per unit area;
θ is the incidence angle;
T is the transmittance;
A is the absorptance;
N is the inward-flowing fraction; and
W_A is the window area.

The quantity (T – NA) is the solar heat gain coefficient (SHGC). Because the optical properties of T and A varies as a function of incidence angle (θ) and wavelength (λ) the SHGC is [7]

$$SHGC(\theta,\lambda) = T(\theta,\lambda) - NA(\theta,\lambda) \tag{1.18}$$

and Equation (1.17) can be written as

$$q_{sol} = E_{DN} \cos(\theta) SHGC(\theta,\lambda) W_A \tag{1.19}$$

In a residential buildings we can assume that the windows are of the clear glass type and therefore not strongly spectrally selective so that the wavelength dependence of SHGC can be neglected. Thus, Equation (1.19) can be re-written as

$$q_{sol} = E_{DN} \cos(\theta) SHGC(\theta) W_A \tag{1.20}$$

Equation (1.20) is the total solar heat gain, at every time step, added to a house and the SHGC (as function of the incidence angle) is given in [7]

$$SHGC(\theta) = T(\theta) - \sum_{k=1}^{L} N_k A_k(\theta) \tag{1.21}$$

where, L is the number of glazing layers, N_k and A_k are the inward-flowing fraction and absorptance of layer k, respectively. Assuming a single layer window, a modified version of Equation (1.21) is

$$SHGC\left(\theta\right)=T\left(\theta\right)-NA\left(\theta\right) \tag{1.22}$$

Since the type of the windows installed in a house is not known a priori; therefore, Equation (1.22) becomes

$$SHGC_e\left(\theta\right)=T\left(\theta\right)-N_eA\left(\theta\right) \tag{1.23}$$

where, N_e (effective N) is an approximation of N and $SHGC_e$ (effective $SHGC$) is an approximation of the $SHGC$. Normally, in order to convert beam radiation measured on one surface to another (i.e., on a tilted surface to that on a horizontal surface) a dimensionless geometric factor; that is, a ratio between the two surfaces is computed and the beam radiation is multiplied by that ratio. For further description of calculating this ratio see [8]. It is further assumed that the orientation and size of the windows is unknown. The objective is to modify Equation (1.20) such that the details of window size and orientation, shading effects, and the fraction of direct or diffuse solar radiation are represented by parameters that can be learned by observation. This eliminates the need for detailed custom configuration by the user. The modified solar heat gain equation is

$$q_{sol}=I\times SHGC_e\left(\theta\right)\times AR_e \tag{1.24}$$

where:

I is the solar irradiance in W/m^2; and

AR_e is an approximation (effective) window area and the ratio of solar irradiance to the vertical surfaces of the windows in units of m^2.

We utilize a moving window optimization technique, described later, to learn the N_e and AR_e parameters.

In order to calculate $SHGC_e$ given in Equation (1.23) the transmittance and absorptance must be calculated based on the angle of incidence. The angle of incidence is calculated using Equation (1.25) described in [8].

$$\begin{aligned}\cos\left(\theta\right)=&\sin\left(\delta\right)\sin\left(\phi\right)\cos\left(\beta\right)-\sin\left(\delta\right)\cos\left(\phi\right)\sin\left(\beta\right)\cos\left(\gamma\right)\\&+\cos\left(\delta\right)\cos\left(\phi\right)\cos\left(\beta\right)\cos\left(\omega\right)+\cos\left(\delta\right)\sin\left(\phi\right)\sin\left(\beta\right)\cos\left(\gamma\right)\cos\left(\omega\right)\\&+\cos\left(\delta\right)\sin\left(\beta\right)\sin\left(\gamma\right)\sin\left(\omega\right)\end{aligned} \tag{1.25}$$

where:

δ is the declination, the angular position of the sun at solar noon;

ϕ is the latitude, the angular location north or south of the equator;

β is the slope, the angle between the plane of the surface in question and the horizontal (windows or solar radiation measuring angle);

γ is the surface azimuth angle, the deviation of the projection on a horizontal plane of the normal to the surface from the local meridian;

ω is the hour angle, the angular displacement of the sun east or west of the local meridian due to rotation of the earth on its axis at 15° per hour; and
θ is the angle of incidence, the angle between the beam radiation on a surface and the normal to that surface.

For a detailed explanation of computation of the values δ, ω, and θ see [8]. While the latitude, slope, longitude, local meridian, local time zone, surface azimuth angle are inputs and based on the geographical location of the NZERTF in Gaithersburg Maryland. The list of inputs and their associated values are given in Table 1.

Table 1. List of inputs and their associated values to calculate the angle of incidence

Inputs	Values based on location of NZERTF
ϕ	39.14°
β (windows tilt $\angle$)	90°
Longitude	77.2°
Local Meridian	75°
Local Time Zone	Eastern
γ	0°

In this application, the incidence angle is computed based on the timestamp associated with the measured data. According to [9], the transmittance and absorptance of a variety of window types can be computed using Equations (1.26) and (1.27).

$$T(\theta)=\sum_{i=0}^{3}c_i\cos^i(\theta) \tag{1.26}$$

$$A(\theta)=\sum_{j=0}^{3}c_j\cos^j(\theta) \tag{1.27}$$

The coefficients c_i and c_j for a single layer glass, $3.2\text{ mm}\,(1/8-inch)$, double strength float are adopted from Table I of [9] and reported in Table 2.

Table 2. Coefficients of a glass window used to calculate transmittance and absorptance

Windows Structure	Solar Properties	c_0	c_1	c_2	c_3
Glass	$T(\theta)$	-0.0372	3.0392	-3.6360	1.4784
	$A(\theta)$	0.0738	0.2370	-0.4364	0.2168

With the transmittance and absorptance calculated, the two unknown parameters are the inward-flowing fraction N_e (from Equation (1.23)) and AR_e (from Equation (1.24)). The total heat gain ($Q_h = q_{sol} + q_{hp} + q_l$) inside the NZERTF with q_{sol} given by Equation (1.24) is

$$Q_h=\left(I\times SHGC_e(\theta)\times AR_e\right)+q_{hp}+q_l \tag{1.28}$$

In order to calculate N_e and AR_e a moving window optimization algorithm was developed and implemented.

2.4 Moving Window Prediction Algorithm

The moving window algorithm utilizes Equations (1.13) and (1.28) to learn the N_e and AR_e parameters from measured data over a training window, the size of which is discussed later. These parameters are then used to predict the next day's indoor temperature. Training is repeated daily using a fixed-size sliding window of data. This approach allows any shading effects and the seasonal variation in sun position to be accounted for. The moving window prediction approach is illustrated in Figure 6. The red rectangles depict the sliding training data window. The green rectangles depict the corresponding prediction horizon.

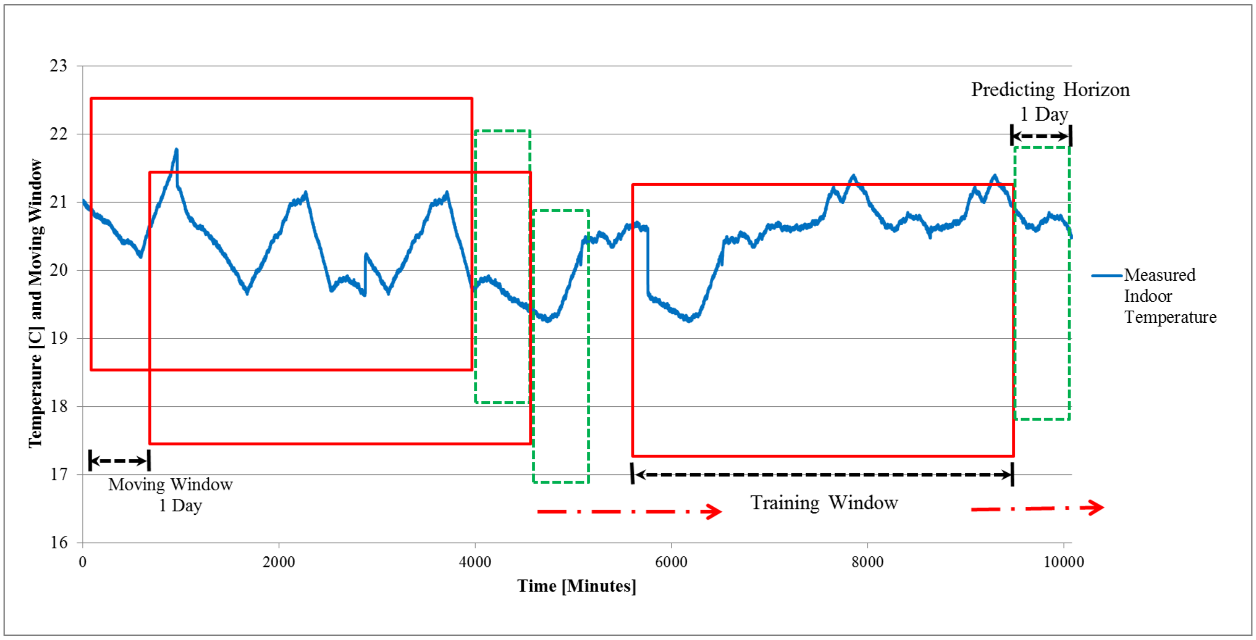

Figure 6. The concept of the moving window prediction algorithm, note that the sizes of the windows are not to scale

The objective function for the moving window algorithm is defined as the SSE between the measured average first floor temperature (T_m) and the predicted temperature (T_p) obtained from Equation (1.13). This can be expressed as

$$f\left(N_e, AR_e\right) = \left\| T_m - T_p \right\|_2^2 \qquad (1.29)$$

The optimization problem is defined as

$$\begin{aligned} \min_{N_e, AR_e} \quad & f(N_e, AR_e) \\ & 0 \le N_e \le 1 \\ & 1 \le AR_e \le \infty \end{aligned} \tag{1.30}$$

where, the N_e is a unitless quantity, and the AR_e is in units of m^2. The upper and lower bounds of the N_e is between [0, 1] because it only represents the fraction of the solar irradiance absorbed into the interior spaces. The lower bound of the AR_e is set to1 for numerical stability. The upper bound is allowed to float because it is not known a priori.

In order to find N_e and AR_e a Matlab non-linear optimization function (*fmincon*) with its default interior-point algorithm was used to minimize Equation (1.30). Initially the algorithm was trained on one day of data and predicted the next day's temperature. But since the N_e and especially AR_e parameters greatly affect the total solar heat gain of the model, the prediction accuracy was highly influenced by the variability of the solar irradiance from one day to the next due to cloud cover. For example, if the parameters were learned on a cloudy day and applied to a day that was sunny the model over predicted the temperature. The model under predicted when the opposite was true. Figure 7 shows the measured solar irradiance for a cloudy training day followed by measured solar irradiance on the prediction day. Figure 8 shows the impact of this situation on predicting the next day's temperature.

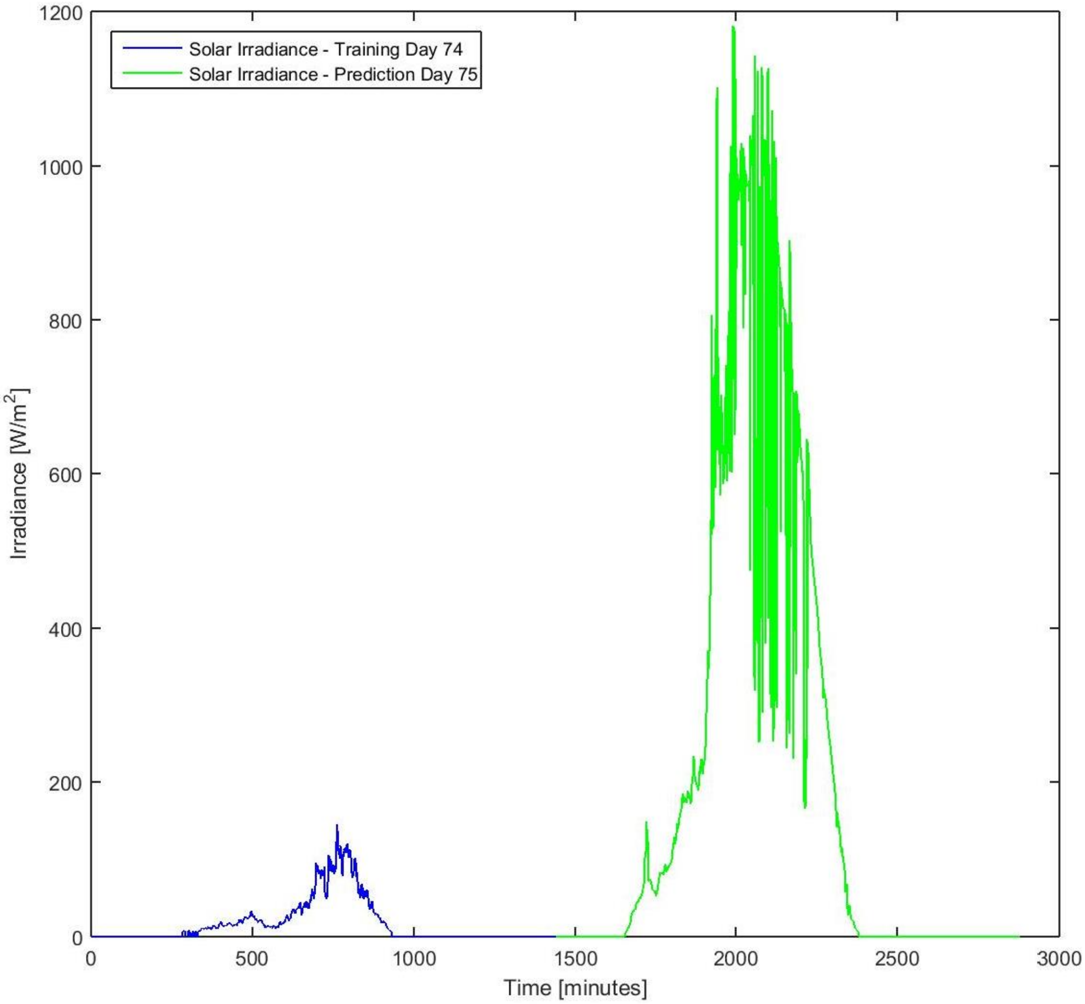

Figure 7. Available solar irradiance – training and prediction days

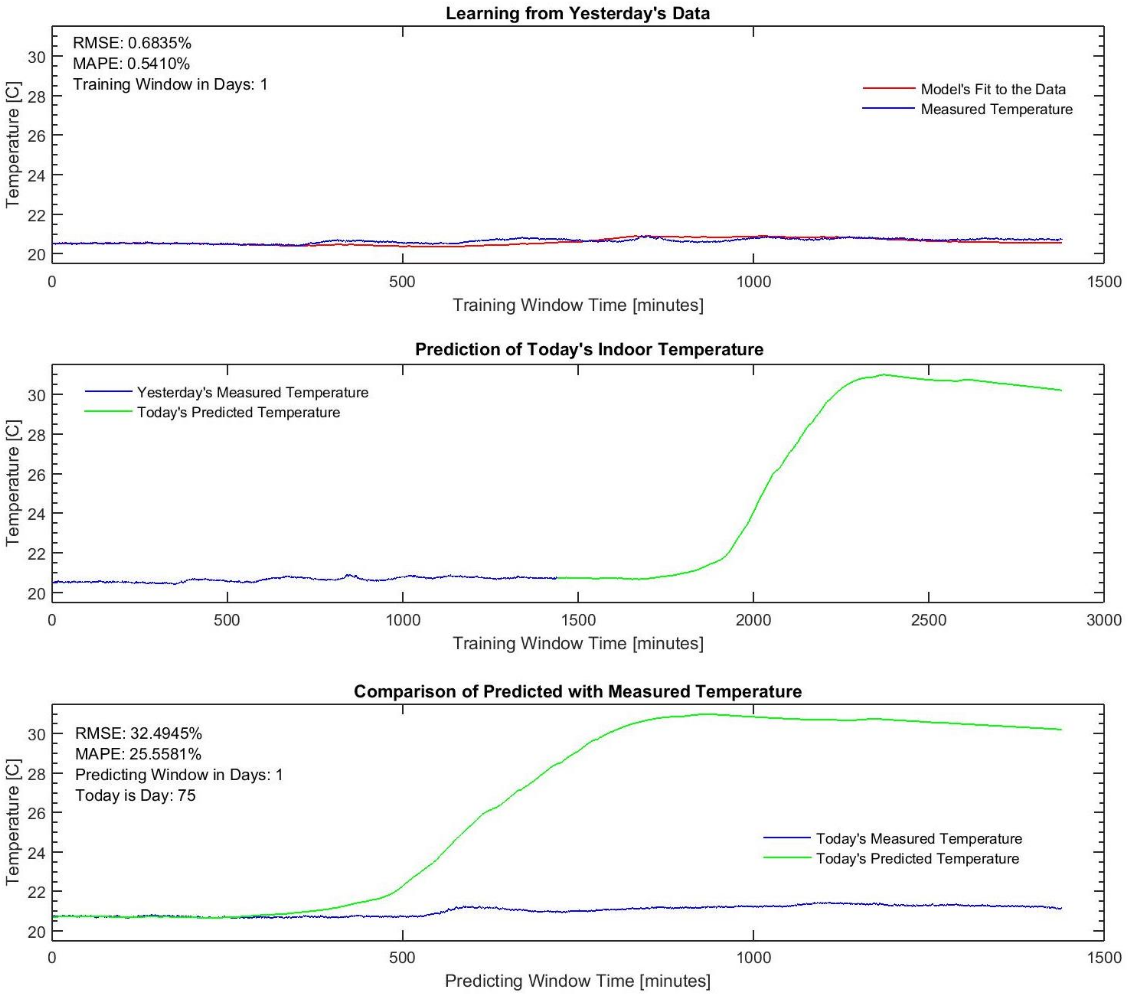

Figure 8. Learning parameters on a cloudy day and applying it to a sunny day (1-day training window)

There is a good agreement between the predicted and measured temperatures, shown in the top plot of Figure 8, because, by adjusting the N_e and AR_e parameters, the learning algorithm minimizes the SSE between the model and the measured data. The second plot shows the model's predicted indoor temperature at the beginning of the day and the third plot shows the comparison between the predicted and the actual measured temperatures for the same day.

It was found that if the parameters were learned on a cloudy or a sunny day and applied to a day with a similar solar condition, the predicted and measured temperatures were close. Figure 9 shows the solar irradiance for the training and prediction days while Figure 10 shows the influence of learning a parameter on such a day and applying it to a day with a similar solar condition.

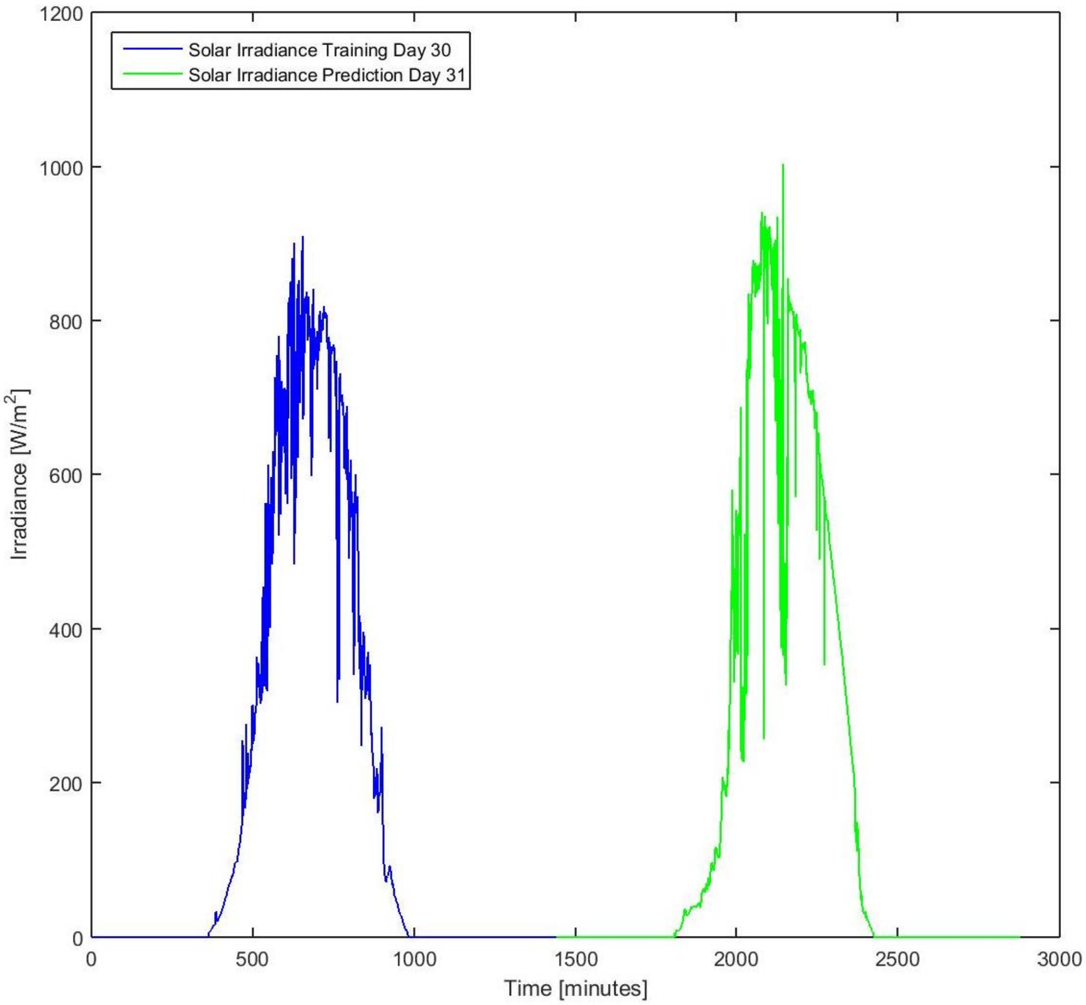

Figure 9. Available solar irradiance – training and prediction days

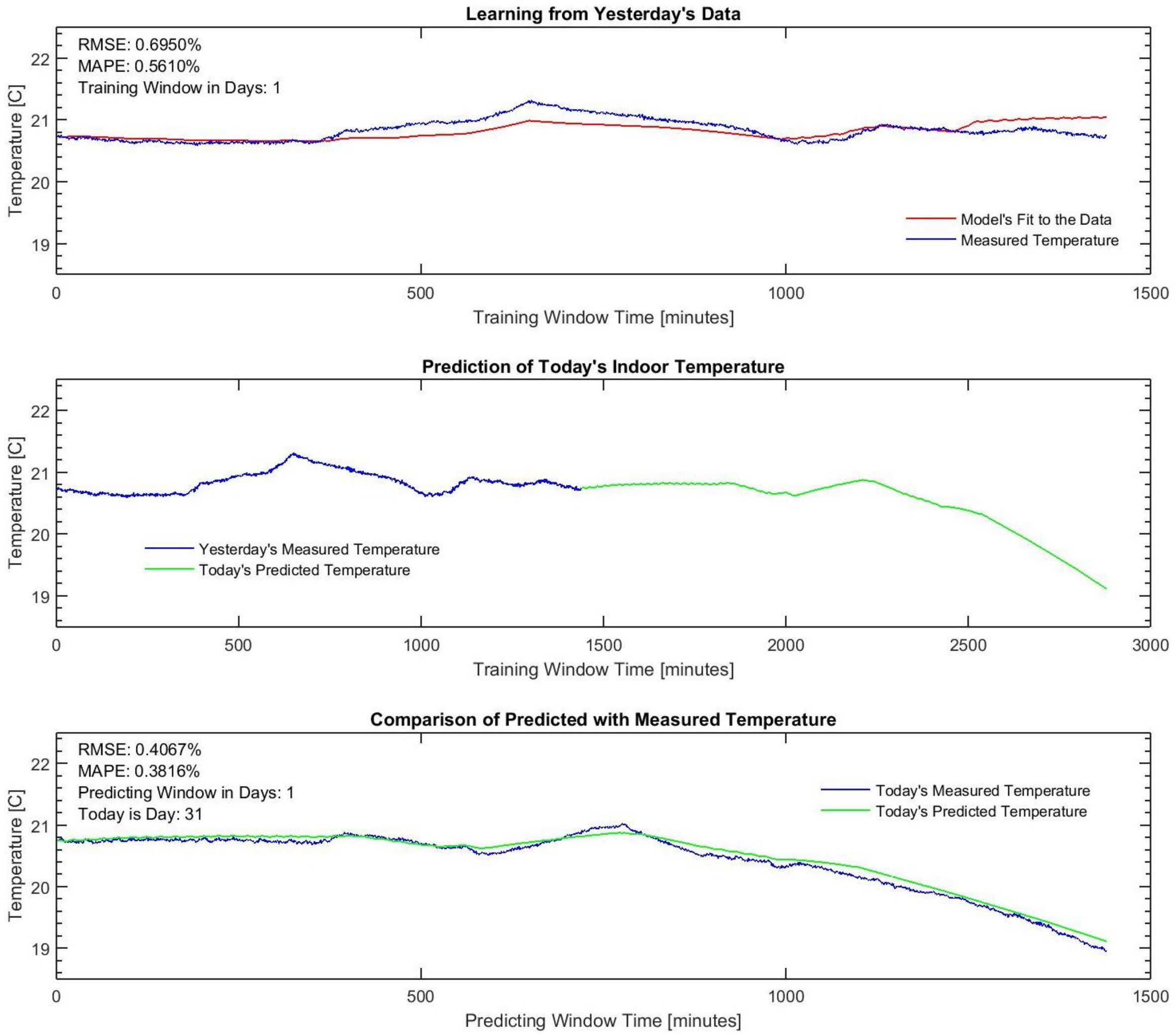

Figure 10. Learning parameters on a sunny day and applying it to a sunny day (1-day training window)

These results clearly indicate that a larger training window is required. In order to evaluate the merit of various training window sizes two statistical measures (relative root mean square error (*% RMSE*) [10] and mean absolute percentage error (*MAPE*) given in [11] are defined as follows

$$\%RMSE = \frac{\sqrt{\dfrac{\sum_{i=1}^{n}\left(T_m^i - T_p^i\right)^2}{n}}}{\overline{T_m}} \times 100 \qquad (1.31)$$

and

$$MAPE = \frac{1}{n}\sum_{i=1}^{n}\left|\frac{T_m^i - T_p^i}{T_m^i}\right| \times 100 \qquad (1.32)$$

where:

n is the number of samples;

T_m^i is the i^th measured temperature;

$\overline{T_m}$ is the mean of the measured temperature; and

T_p^i is the i^th predicted temperature.

Both *% RMSE* and *MAPE* are dimensionless quantities, and a measure of closeness of the predicted and measured temperatures. The output of Equation (1.31) and (1.32), reported in Table 3, confirms the observation that the prediction accuracy of the model is significantly improved when the training and prediction days had identical solar conditions.

Table 3. Prediction horizon *% RMSE* and *MAPE* (1-day training window)

Figure #	% *RMSE*	*MAPE*
Figure 8	29	23
Figure 10	0.4	0.4

Using these metrics an optimal window size can be determined. The prediction algorithm was tested for various training window sizes over the 85-days data set. The average *% RMSE*, for each training window size, was calculated and reported in Figure 11. Figure 11 also shows the average elapsed time (in minutes) that the optimization algorithm took while learning the N_e and AR_e parameters. It is noted that the elapsed time is specific to our implementation of the algorithm. Faster times may be possible but in general the larger the training window the slower the optimization.

Figure 11 shows that there is large reduction in *% RMSE* when the size of the training window is increased from 1 to 3 days. The error is further reduced, gradually, until the size of the training window is 7 days long. There is a slight increase in the error for the 14 and 21 days of training, however the increase is minimal. Even though the 42 days training window has the lowest *% RMSE*, the time that the optimization requires to learn N_e and AR_e is significantly larger compared to the rest of the training windows. Considering the elapsed times, number of training data required, and smaller prediction error, it was decided that the 7-day training window was an appropriate size.

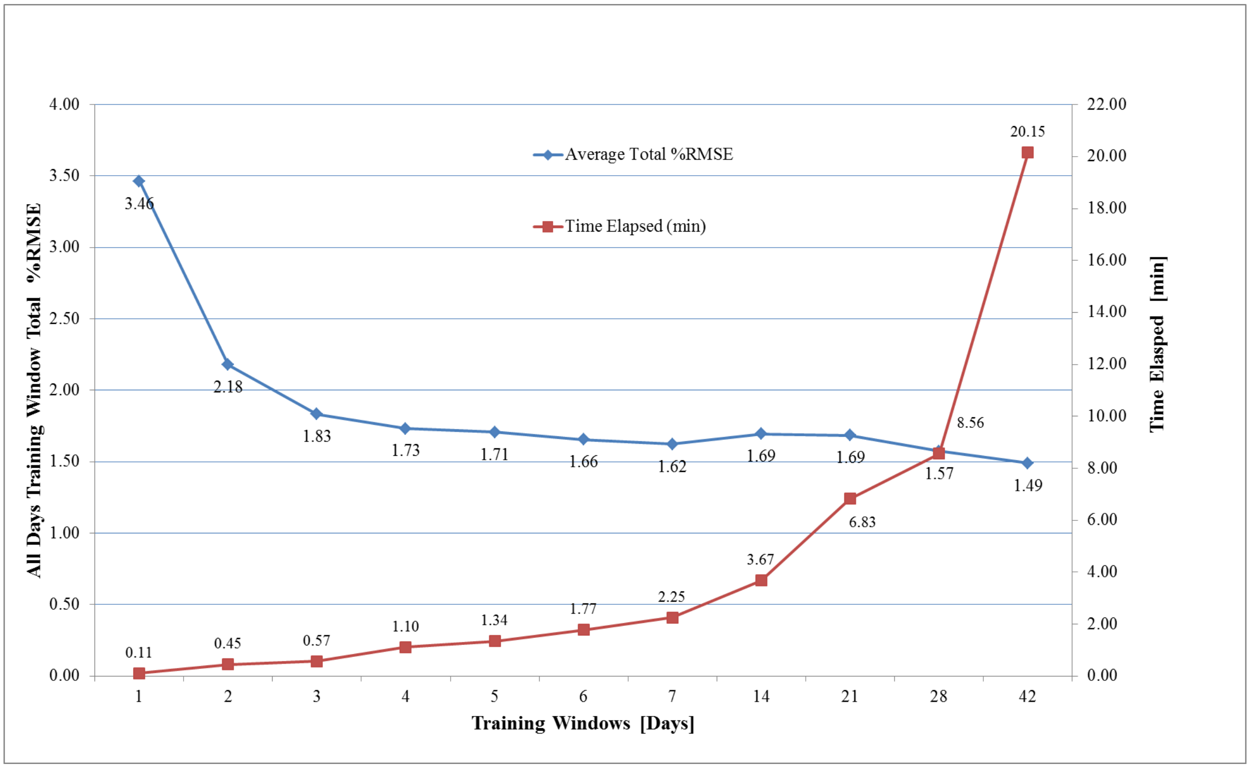

Figure 11. Average *% RMSE* for various training window sizes (UA_e = 172 W/K and τ_e = 104 h)

The impact of using the seven-day vs. one-day of training is shown for the same days, previously depicted in Figure 8 and Figure 10, are given in Figure 12 and Figure 13, respectively.

The *% RMSE* and *MAPE* shown in Figure 12 have significantly improved over the values reported, for the same days, in Figure 8. However, the *% RMSE* and *MAPE* shown in Figure 13 have slightly increased over the same days reported in Figure 10. The slight increase in *% RMSE* and *MAPE* were expected because the N_e and AR_e parameters were effectively average values vs. a day where the solar conditions were similar to the conditions of the day being predicted.

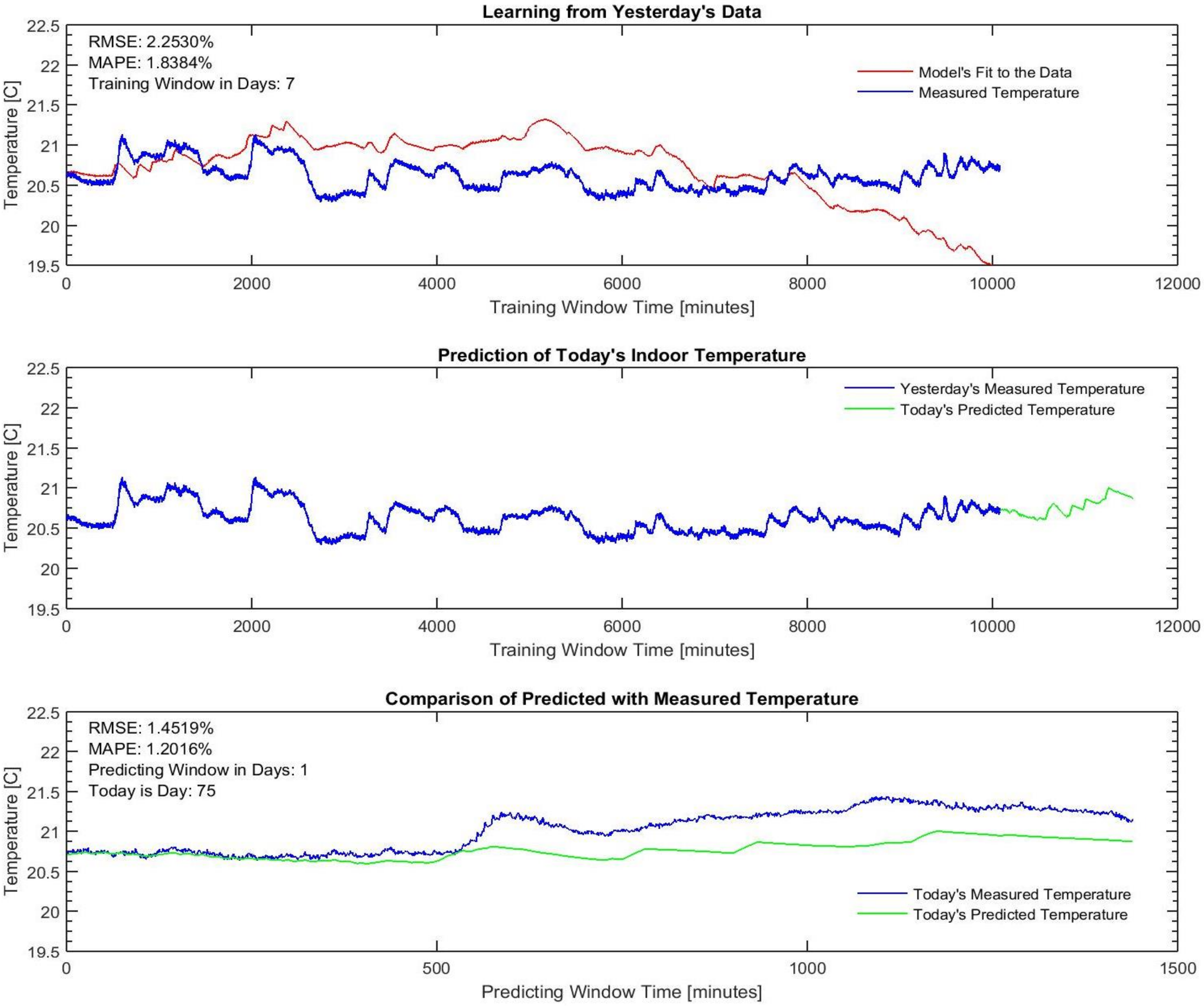

Figure 12. Learning parameters over a 7-day training window and applying to a sunny day

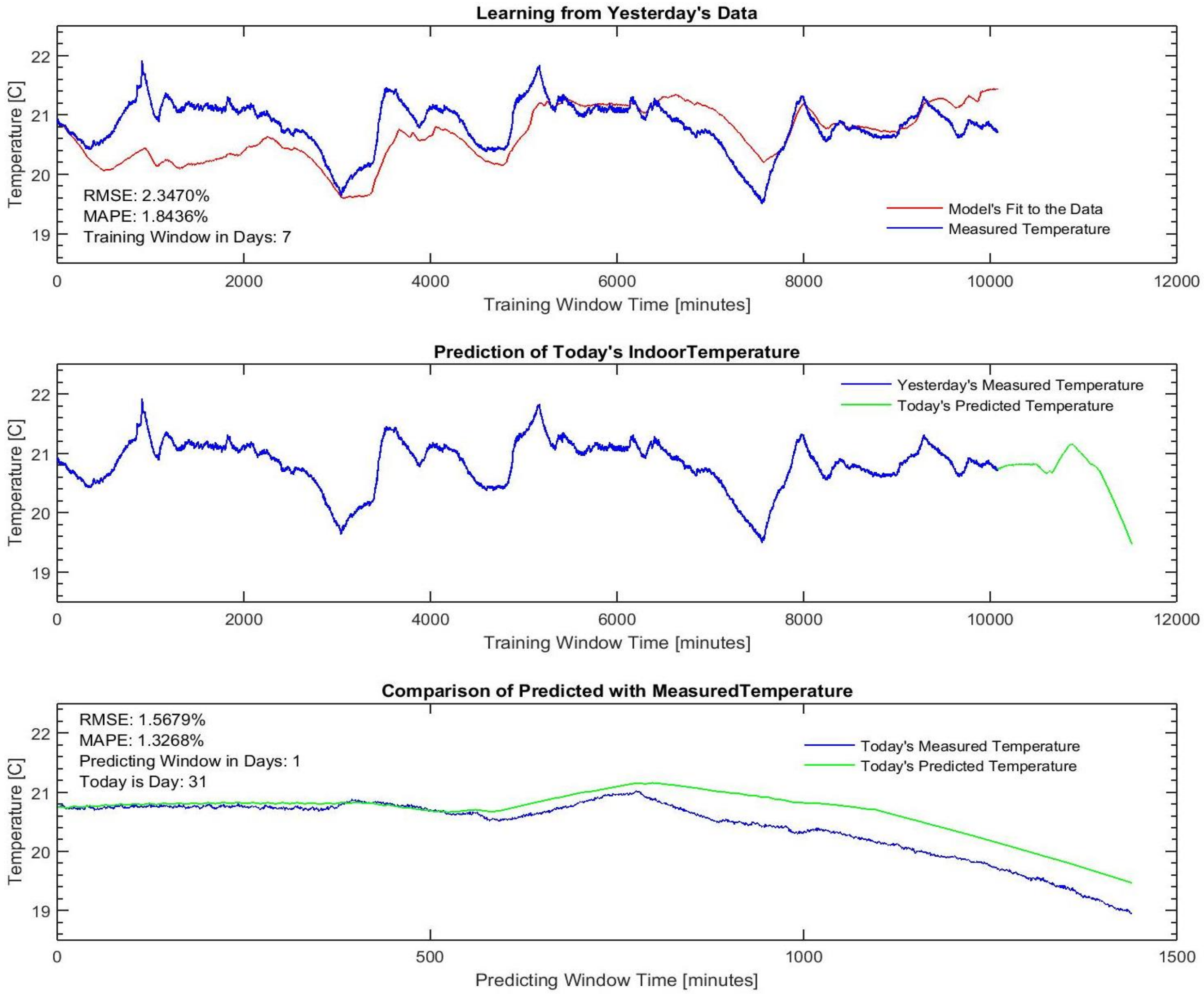

Figure 13. Learning parameters over a 7-day training window and applying it to a sunny day

The maximum *% RMSE* and *MAPE* errors, for a one-day training window, over 85-day data set are 33 % and 26 %, respectively. The corresponding maximum *% RMSE* and *MAPE* errors, for the seven-day training window, are 7 % and 5 %, respectively. The *% RMSE* and *MAPE*, for seven-day training window, and their average errors are shown in Figure 14.

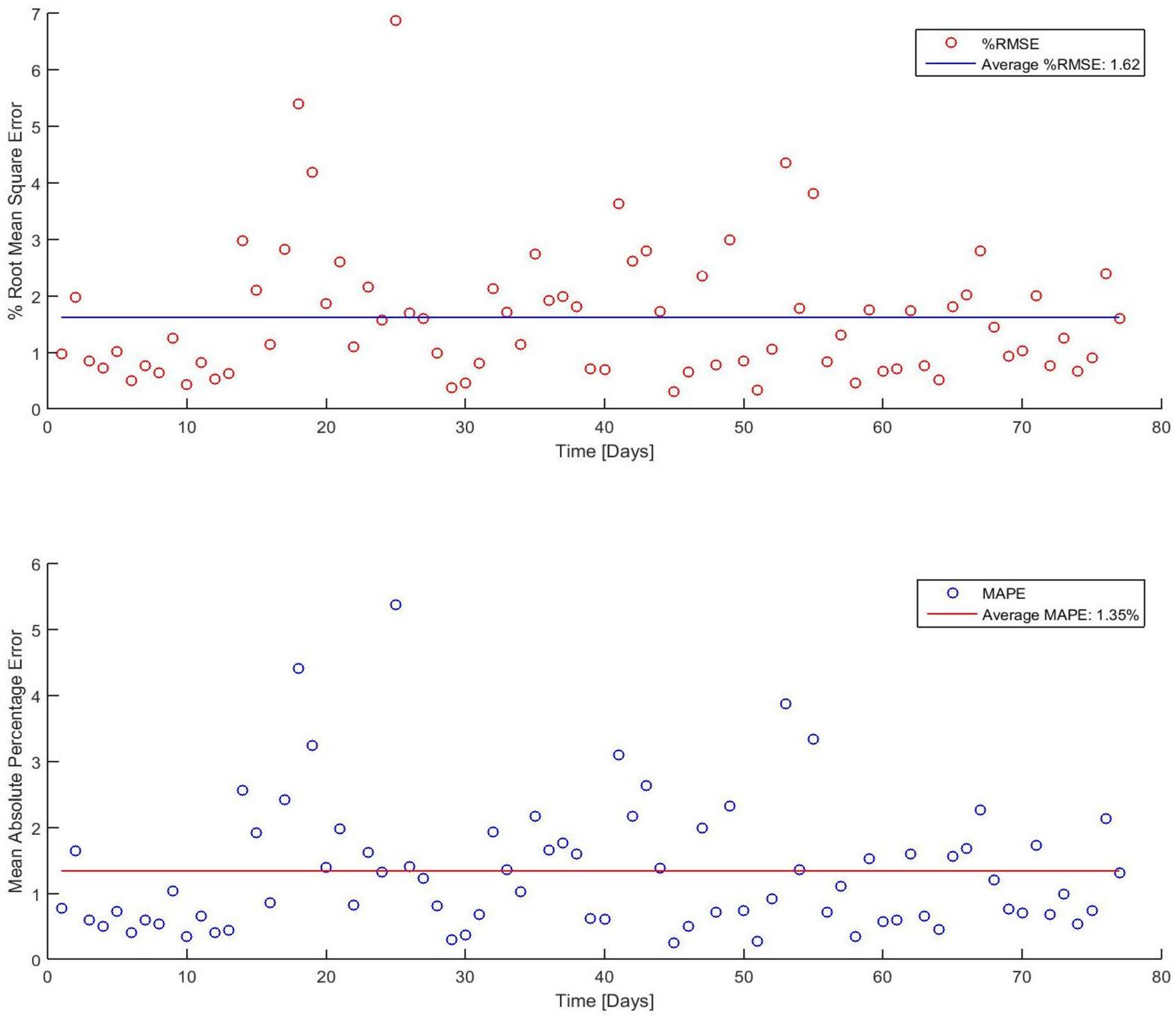

Figure 14. The % RMSE, MAPE and the average error for both metrics (7-day training window)

In order to visually depict the behavior of the learning algorithm and its prediction capabilities, three different prediction scenarios were identified to represent the worst (Figure 15), a typical (Figure 16), and the best case (Figure 17).

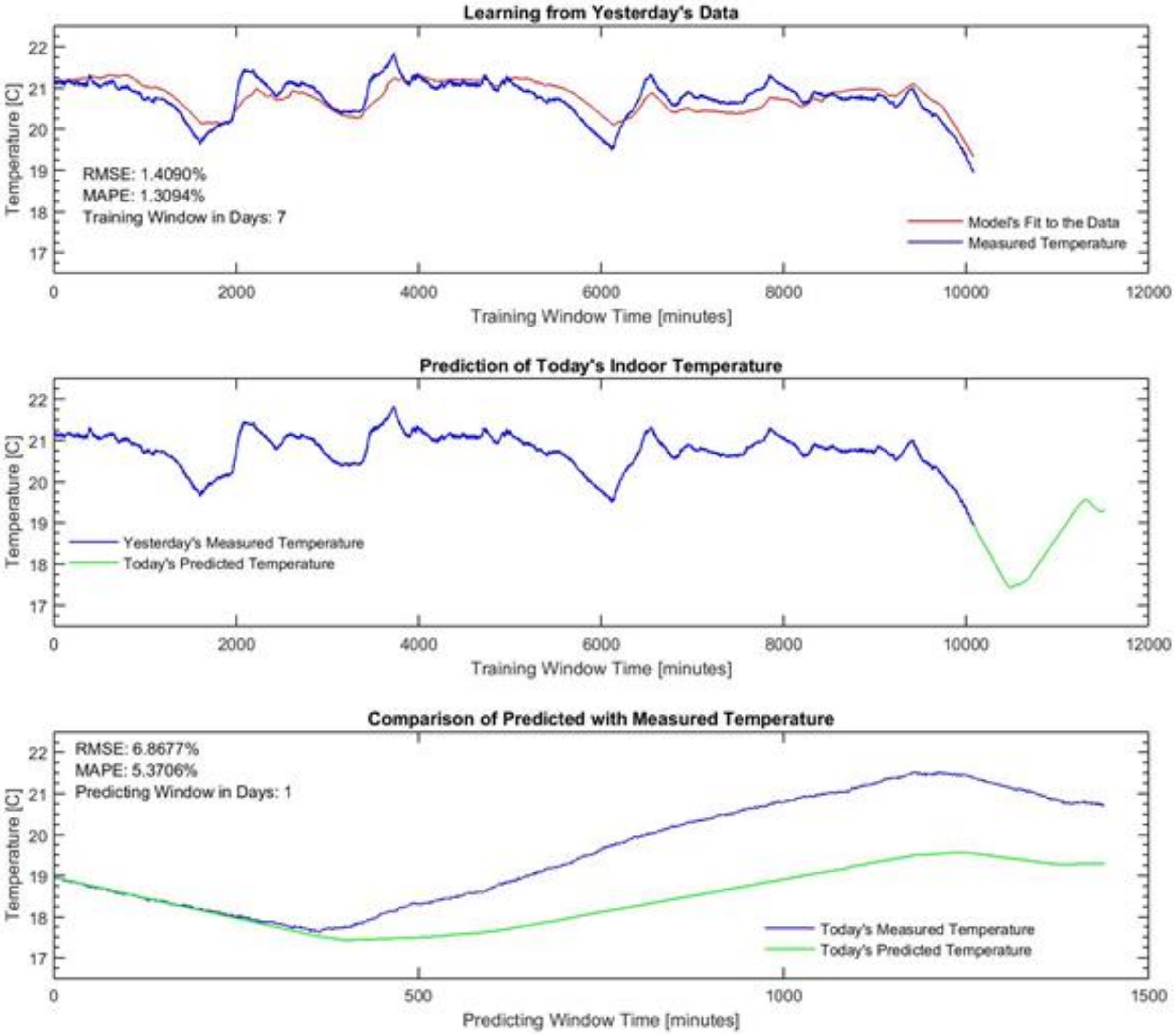

Figure 15. The worst case prediction scenario (7-day training window)

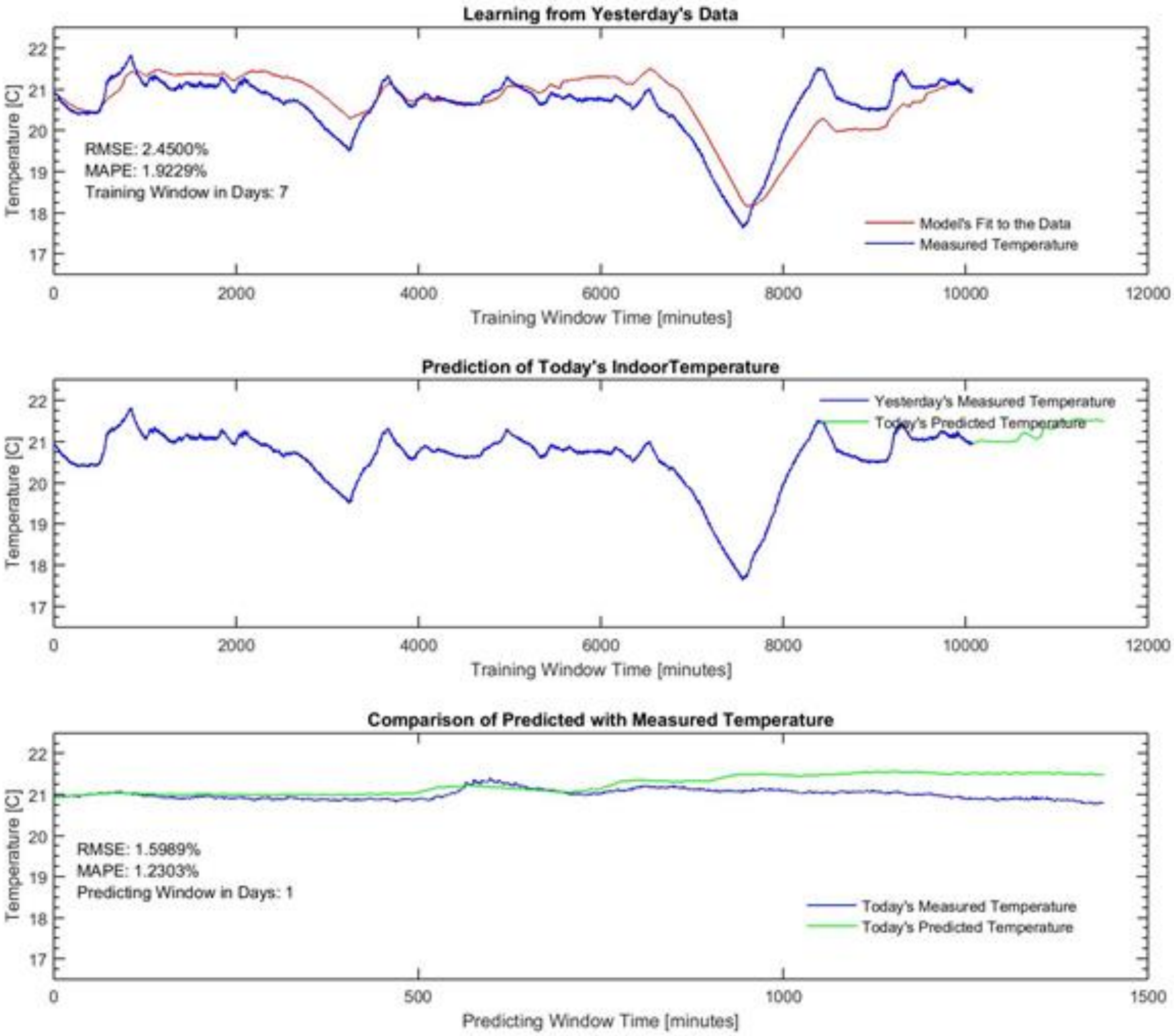

Figure 16. A typical case prediction scenario (7-day training window)

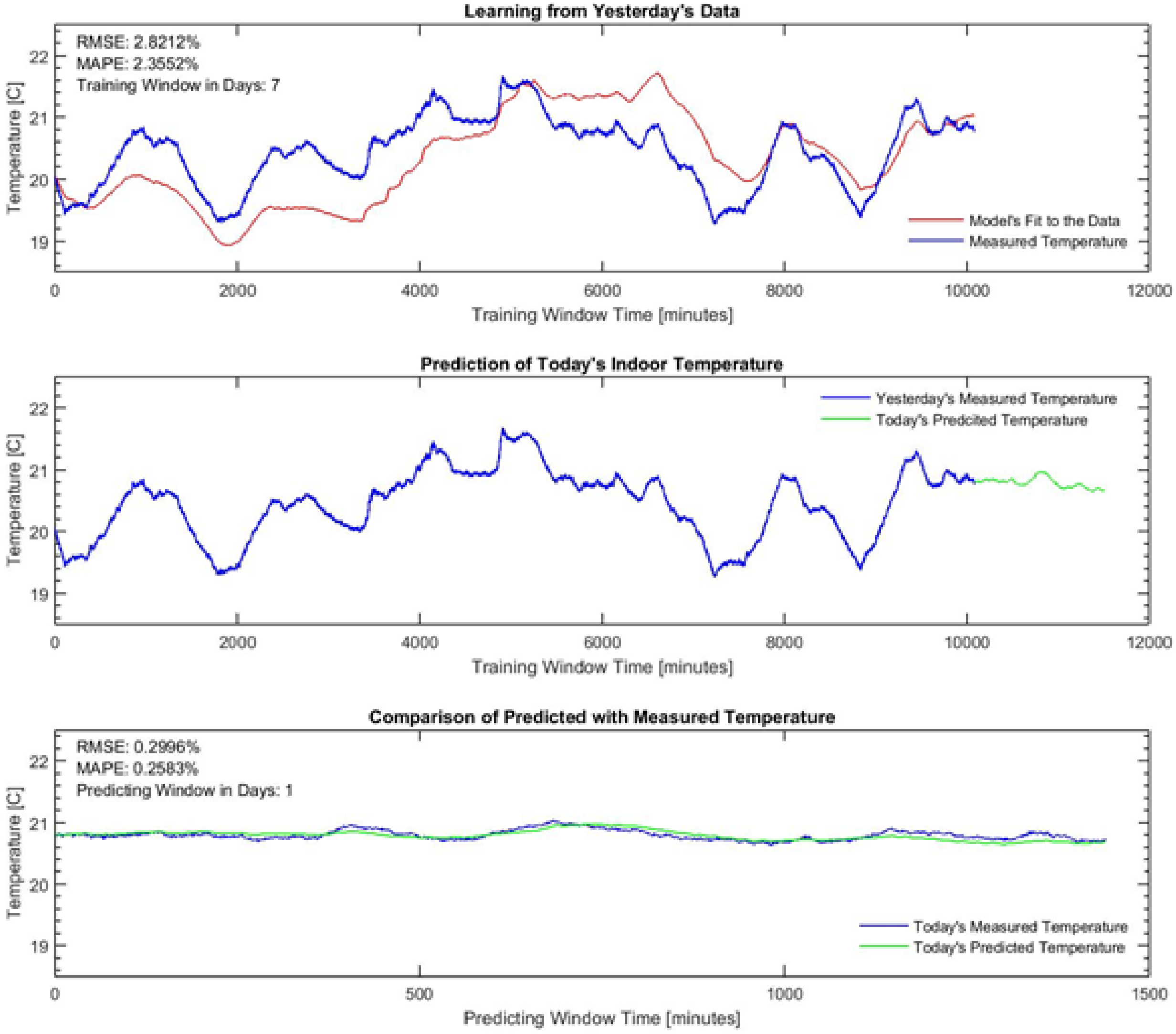

Figure 17. The best case prediction scenario (7-day training window)

4. Conclusion and Future Work

In order to develop effective control optimization strategies to manage residential electricity consumption in a smart grid environment, predictive algorithms are needed that are simple to implement, minimize custom configuration, and provide enough accuracy to enable meaningful control decisions. A self-learning algorithm for predicting indoor temperature changes is derived using a first-order lumped capacitance technique. The algorithm is formulated in such a way that key design details such as window size and configuration, thermal insulation, and airtightness that effect heat loss and solar heat gain are combined into effective parameters that can be learned from observation. This eliminates the need for custom configuration for each residence.

Using experimental data from the NZERTF, it was demonstrated that an effective overall head transfer coefficient UA_e and thermal time constant τ_e for the house can be learned from a single nighttime temperature decay test. On a winter night the temperature setpoint was lowered to permit a larger than normal drop in indoor temperature and the temperature decay over time was measured. A least squared error fit to the data was used to determine UA_e and τ_e. The resulting value of UA_e was verified by using an alternate technique.

The effect of solar irradiance on indoor temperature was accounted for by defining an effective solar heat gain coefficient $SHGC_e$ and a parameter AR_e that combines the unknown window area with the unknown ratio of solar irradiance measured on a horizontal surface to the solar irradiance normal to the windows. A sliding-window learning algorithm was developed that can learn these parameters from a combination of solar irradiance data, internal temperature data, and the previously estimated UA_e and τ_e. The sliding window of learning data accounts for both seasonal variations in the sun position and daily cloud cover fluctuations. By trial and error, using data from the NZERTF, it was determined that a training window size of seven days produced good results.

The resulting algorithm was verified using 85 days of performance data from the NZERTF. After a seven day learning period, the algorithm was used each day to predict a one-day temperature profile using known solar irradiance measurements as a forecast and known heat pump thermal energy output. The predicted temperature profile agreed with measured values with an average root mean square error of 2 % and a maximum root mean square error of 7 % over the 85-day period. A maximum absolute percentage error analysis was done on the same data resulting in an average error of 1 % and a maximum error of 5 %.

Application of the algorithm requires a forecast of solar irradiance and outdoor temperature. It also requires past measurements of indoor temperature, outdoor temperature, and thermal energy output from heating and cooling equipment. The learning process eliminates the need for additional construction detail information for the residence. It is expected that the temperature prediction algorithm is sufficiently accurate to enable a control optimization algorithm to predict the effect of alternate control strategies for operating HVAC equipment on occupant comfort in a smart grid environment where electricity price changes with time of year and grid conditions.

Additional work is planned to verify that the algorithm and training window size are broadly applicable to single family residences and to determine the potential impact of combining it with user-defined comfort constraints to reduce electricity costs in a smart grid environment.

References

[1] IBPSA-USA, “Best Directory | Building Energy Software Tools.” [Online]. Available: http://www.buildingenergysoftwaretools.com/. [Accessed: 15-Aug-2015].

[2] H. Fanney, V. Payne, T. Ullah, N. Lisa, M. Boyd, F. Omar, M. Davis, H. Skye, B. Dougherty, B. Polidoro, W. Healy, J. Kneifel, and B. Pettit, “Net-zero and Beyond! Design and Performance of NIST’s Net-zero Energy Residential Test Facility,” *Energy Build. 101*, pp. 95–109, 2015.

[3] F. Omar and S. Bushby, “Simulating Occupancy in the NIST Net-Zero Energy Residential Test Facility,” NIST, Technical Note 1817, 2013.

[4] F. Incropera and D. DeWitt, “Introduction to Heat Transfer,” 4th ed., Wiley, 2002, pp. 240–249.

[5] M. Davis, W. Heally, M. Boyd, L. Ng, V. Payne, H. Skye, and T. Ullah, “Monitoring Techniques for the Net-Zero Energy Residential Test Facility,” NIST, Technical Note 1854, 2014.

[6] “Chapter 15. Fenestration,” in *ASHRAE Handbook: Fundamentals*, ASHRAE, 2013, p. 13.

[7] “Chapter 15. Fenestration,” in *ASHRAE Handbook: Fundamentals*, ASHRAE, 2013, p. 17.

[8] J. A. Duffie and W. A. Beckman, “Solar Radiation,” in *Solar Enginieering of Thermal Processes*, 3rd ed., Wiley, 2006, pp. 3–17.

[9] M. Rubin, “Solar optical properties of windows,” *Energy Res.*, vol. 6, pp. 123–133, 1982.

[10] P. Lei, “A Linear Programming Method for Synthesizing Origin-Destination (O-D) Trip Tables from Traffic Counts for Inconsistent Systems,” Virginia Polytechnic Institute and State University, 1998.

[11] J. S. Armstrong, Ed., “Appendix,” in *Principle of Forecasting: A Handbook for Researchers and Practitioners*, Kluwer Academic Publishers, 2001, p. 470.